Falling film evaporation and pool boiling heat transfer of R1233zd(E) on thermal spray coated tube

Ubara, Tsutomu
Asano, Hitoshi
Sugimoto, Katsumi

(Citation)
Applied Thermal Engineering,196:117329

(Issue Date)
2021-09

(Resource Type)
journal article

(Version)
Accepted Manuscript

(URL)
https://hdl.handle.net/20.500.14094/90008548

Title.

Falling Film Evaporation and Pool Boiling Heat Transfer of R1233zd(E) on Thermal Spray Coated Tube

Author names and affiliations.

Tsutomu UBARA [a, *]

195t310t@stu.kobe-u.ac.jp,

Hitoshi ASANO [a]

asano@mech.kobe-u.ac.jp

Katsumi SUGIMOTO [a]

sugimoto@mech.kobe-u.ac.jp

[a] Department of Mechanical Engineering, Graduate School of Engineering, Kobe University

1-1, Rokkodai, Nada, Kobe 657-8501, Japan

***Corresponding author.**

Tsutomu UBARA

E-mail address: 195t310t@stu.kobe-u.ac.jp

Phone/FAX number: +81-78-803-6122

Highlights

- Falling film evaporation heat transfer of R1233zd(E) was experimentally investigated.
- Up to 4.2-fold heat transfer enhancement could be obtained by thermal spray coating.
- R1233zd(E) achieved a lower heat transfer coefficient than R134a at 20 °C.

Abstract

Falling film evaporators have been expected as an alternative to flooded evaporators for reducing the refrigerant usage. It is important for the enhancement of the film evaporation heat transfer to keep a liquid film and promote nucleate boiling in the liquid film. This study focused on nucleate boiling heat transfer in the liquid film by thermal spray coating that can be applied regardless of the material of heat transfer tubes. The heat transfer performance of falling film evaporation on a horizontal copper tube was experimentally evaluated. Since nucleate boiling phenomena, such as activation of nucleation sites and bubble behaviors in the liquid film, strongly depend on the physical properties of the refrigerant, the experimental results for R1233zd(E), one of the alternative refrigerants with low GWP, were compared with those for R134a. Two types of tubes were used: the smooth tube and the thermal spray coated tube fabricated by an arc wire spraying method, with the outer diameter of 19.05 mm and the heating length of 50 mm. Pool boiling experiments were also conducted to confirm the wall superheat for nucleate boiling. The heat transfer coefficients were evaluated with a film mass flow rate range of 8.5×10^{-3} to 6.3×10^{-2} kg/(m·s), a heat flux range of 10 to 85 kW/m^2, and a saturation temperature at 20 °C. The effects of the structure of the heating surface, heat flux, and thermophysical properties of the refrigerant on the heat transfer performance are discussed. Results show that the heat transfer of the falling film became the nucleate boiling dominant with a sufficient heat flux and liquid film flow rate. The thermal spray coated surface enhanced not only the nucleate boiling but also the liquid spreading by the vapor bubbles in the liquid film, and thus the coated tube produced higher heat

transfer coefficients of 2.1 to 4.8 times those for the smooth tube. The wall superheat at the onset of nucleate boiling was higher for R1233zd(E) than for R134a, because R1233zd(E) has a higher surface tension and lower vapor density. Thus, the pool boiling and falling film evaporation heat transfer coefficients were lower for R1233zd(E) than for R134a.

Key words

Falling film evaporation, Thermal spray coating, R1233zd(E), Pool boiling, Heat transfer enhancement, Nucleate boiling

Nomenclature

C	parameter in Eq. (6)	[-]
c_p	specific heat at constant pressure	[J/(kg·K)]
D	outer diameter	[m]
D_b	bubble departure diameter	[m]
g	gravitational acceleration	[m/s^2]
i	latent heat of evaporation	[J/kg]
L	heating length	[m]
$\dot{m}$	mass flow rate	[kg/s]
P	pressure	[Pa]
$\dot{Q}$	heating rate	[W]
$\dot{q}$	heat flux	[W/m^2]
Ra	average roughness	[μm]
Rz	maximum height of profile	[μm]
r	radius of cavity	[m]
T	temperature	[K]

Greek symbols

α	heat transfer coefficient	[W/(m^2·K)]
Γ	mass flow rate of liquid film	[kg/(m·s)]
λ	thermal conductivity	[W/(m·K)]
μ	viscosity	[Pa·s]
ρ	density	[kg/m^3]

σ	surface tension	[N/m]

Subscripts

crt	critical
L	liquid
min	minimum
red	reduced parameter
sat	saturation
V	vapor
wall	heat transfer surface

1 Introduction

As most hydrofluorocarbon (HFC) refrigerants have a high global warming potential (GWP), a reduction in refrigerant charges and a shift to low-GWP refrigerants are important issues. Falling film evaporators are expected to be substitutes for typical flooded evaporators because they can operate with less refrigerant. In addition, falling film evaporators have advantages, such as a low pressure drop and high heat transfer coefficient, and thus are applicable to refrigeration, air conditioning, waste heat recovery, and chemical processes.

Experimental studies on falling film evaporation using water, ammonia, and fluorocarbon refrigerants have been conducted, and an overall review was carried out by Ribatski and Jacobi [1] in 2005. In falling film evaporation, the refrigerant flow rate is an important parameter because it strongly affects the wetting area on the heat transfer tubes. A wide and thin liquid film is required to obtain a high heat transfer coefficient.

When fluorocarbon refrigerants with a low surface tension are used as the working fluid, strong evaporation and nucleate boiling occur at a high heat flux, and dry patches leading to heat transfer deterioration are formed. Therefore, the liquid flow rate should be increased to avoid dry patch formation. However, Fujita and Tsutsui [2] reported that such dry patches do not immediately lessen the heat transfer coefficient because dry patches move randomly on the heat transfer surface. After the dry patches are established and become predominant on the heat transfer surface, the heat transfer coefficient decreases significantly [3, 4]. In contrast, under well-wetted conditions with sufficient

liquid supply, the effect of the liquid flow rate on the heat transfer coefficient is small. The flow and heat transfer conditions are called the plateau region [5, 6].

Nucleate boiling plays a significant role in the falling film evaporation heat transfer of fluorocarbon refrigerants. Without dry patches on the heat transfer surface, the heat transfer of the falling film is forced convection dominant at a low heat flux, whereas it becomes nucleate boiling dominant at a high heat flux [7]. The transition from forced convection to nucleate boiling is strongly related to the onset of nucleate boiling (ONB); thus, the heat transfer of the falling film is expected to be enhanced by promoting nucleate boiling in the liquid film.

The most effective method for nucleate boiling heat transfer enhancement is to increase the nucleation site density using cavities. Complex machining processes are usually applied to the outer walls of heat transfer tubes. However, it is difficult to apply such a machining process in certain applications using corrosion-resistant tubes, such as stainless steel and Inconel tubes, in an evaporator. Since these materials are difficult to cut into fine structures, other heat transfer enhancement methods onto the tube surface are required.

This study focused on a thermal spray coating method because it is a relatively simple process and can be easily applied to hard materials. A melted spraying material was sprayed to form a coating layer. Previous pool boiling experiments using refrigerants confirmed that the fine porous structure of the coating layer enhanced the nucleate boiling heat transfer [8, 9]. On examining nucleate boiling heat

transfer for a porous coated surface, Tehver et al. [10] reported a large hysteresis effect in their pool boiling experiments using a plasma-sprayed surface.

Several studies have been conducted on the enhancement of falling film evaporation heat transfer by porous structures, but most of them used water as the working fluid without boiling. Abraham and Mani [11] carried out experiments on plain and thermal spray coated aluminum tubes using water as the working fluid. The heat transfer coefficients were improved by 20%–30% through the coating because of the increase in the turbulent intensity and the decrease in the film thickness. Bogan and Park [12] studied the falling film evaporation of distilled water at a saturation temperature of 60 °C on a porous surface structure made by sintering copper particles with a mean diameter of 75 μm. They evaluated the sensible and evaporation heat transfers separately and found that the evaporation heat transfer was higher on the porous surface tube than on the smooth tube. Other studies have been summarized by Abed et al. [13] in 2015.

For a fluorocarbon refrigerant, nucleate boiling enhancement in the liquid film appears significantly. Ubara et al. [14] investigated the heat transfer enhancement effect of thermal spray coating using R134a at a saturation temperature of 20 °C. A copper tube with an outer diameter of 19.05 mm was thermal spray coated using copper as the spraying material. The results showed that the coated tube achieved up to a 5.2-fold higher heat transfer than a smooth tube. However, the heat transfer enhancement effect of thermal spray coating for other refrigerants with different thermophysical properties is still unclear.

The heat transfer performance depends not only on the structure of the heat transfer surface, but also on the thermophysical properties of the refrigerants. Even for the same heat transfer enhancement tube, the heat transfer coefficients and enhancement factors depend on the type of refrigerant. Zhao et al. [5] investigated the falling film evaporation heat transfer of R134a and R123 on four types of mechanically processed tubes at a saturation temperature of 6 °C. The heat transfer tube that produced the highest heat transfer differed between the two refrigerants. A larger opening of the reentrant cavity was effective for R134a and a smaller opening for R123; however, further study is needed to clarify the reason. Chien and Tsai [15] investigated the falling film evaporation heat transfer of R245fa and R134a on a low finned tube with and without a covering of brass mesh at a saturation temperature of 20 °C. The fin height was 0.4 mm with 60 fins per inch. The mesh was made of ϕ 0.09 mm wire with 100 mesh per inch. By wrapping the low finned tube with mesh, the heat transfer was improved for R245fa and deteriorated for R134a. It has been reported that the main reason might be the difference in the specific volume of vapor.

Recently, new-generation refrigerants with low GWP have been developed, and their heat transfer performances have been attracting attention. R1233zd(E) is an alternative refrigerant for relatively low-pressure or high-temperature applications, including binary power generation and waste heat recovery heat pump systems. Several recent studies have experimentally investigated the pool boiling heat transfer characteristics of R1233zd(E) [16–19]. Nagata et al. [16] investigated the pool boiling heat transfer of R1234ze(E), R1234ze(Z), and R1233zd(E) on a smooth tube at saturation temperatures

of 10, 40, and 60 °C. The experimental results were compared with those of R245fa and R134a. The heat transfer coefficient of R1233zd(E) was significantly lower than that of R134a, but slightly lower than that of R245fa at the same saturation temperature. Byun et al. [17] investigated the pool boiling heat transfer of R1234ze(E) and R1233zd(E) on one smooth and two mechanically processed tubes at saturation temperatures of 4.4 °C and 26.7 °C. Ji et al. [18] also investigated the pool boiling heat transfer of R1234ze(E), R1233zd(E), and R134a on two mechanically processed boiling enhancement tubes at a saturation temperature of 6 °C. In both studies, the heat transfer coefficients of R1233zd(E) were lower than those of R134a, even on the enhancement tubes.

In contrast to pool boiling experiments, there have been few studies on the falling film evaporation of R1233zd(E) on a single horizontal tube, targeting the condition in a shell-and-tube evaporator. Hassani and Kouhikamali [20] conducted a 2D numerical simulation of falling film evaporation on a smooth tube considering nucleate boiling. Numerical studies are effective for evaluating the differences in the heat transfer performance using various fluids. For an accurate evaluation, complex 3D phenomena, such as dry patch formation and bubble nucleation on the heat transfer surface, should be considered. Wang et al. [21] reviewed that previous studies on the numerical simulation of falling film evaporation have rarely involved boiling simulations. Experimental evaluations are still needed to clarify the falling film heat transfer characteristics with nucleate boiling on smooth and processed tubes, particularly the effect of the thermophysical properties.

178 The purpose of this study is to experimentally investigate the falling film evaporation heat transfer
179 characteristics of R1233zd(E) and the heat transfer enhancement effect of thermal spray coating,
180 focusing on nucleate boiling heat transfer in a falling liquid film. A porous coating processed by the
181 thermal spraying of copper was applied to the heat transfer surface. The heat transfer performance of
182 falling film evaporation and pool boiling on a single horizontal copper tube with an outer diameter of
183 19.05 mm was evaluated at a saturation temperature of 20 °C. Pool boiling experiments were
184 conducted to confirm the wall superheat required for nucleate boiling. The effects of the
185 thermophysical properties were considered by comparing the results with those for R134a reported by
186 Ubara et al. [14].

187 **2 Experimental methods**

188 **2.1 Experimental apparatus**

189 A schematic diagram of the experimental apparatus is shown in Fig. 1. The details were reported
190 by Ubara et al. [14]. The inside of the apparatus was first evacuated and then filled with the working
191 fluid. Both the falling film evaporation and pool boiling experiments were carried out in a pressure
192 vessel by changing the liquid level.

193 In the falling film evaporation experiments, the liquid level was set below the test section. The
194 refrigerant liquid was circulated by a gear pump and supplied from three needle nozzles above the test
195 section. The nozzle length was 22 mm, the inner diameter was 1.48 mm, and it was attached at the
196 bottom of a horizontal copper tube. The liquid temperature was maintained using a subcooler. The flow

resistance of the nozzle was sufficiently high for uniform flow distribution. A heat transfer enhancement tube with microgrooves on the outer surface (GEWA-B5H produced by Wieland) was set just above the test section to spread the liquid in the axial direction. The gap between the dummy tube and test tube was set to 1 mm to form a stable and homogeneous liquid film. Both tubes were carefully installed horizontally to prevent a maldistribution due to gravity. The mass flow rate of the refrigerant was measured using a Coriolis mass flow meter. The flow rate was maintained by the rotational speed of the pump and the opening of the valve on the bypass line. The supplied liquid temperature was measured using a K-type thermocouple just upstream of the liquid-supplying nozzles. In the pool boiling experiments, nozzles and a dummy tube were removed, and the test section was submerged in the liquid pool.

The generated refrigerant vapor was condensed in a double tube condenser connected to the upper part of the pressure vessel, and the condensed liquid returned to the vessel by gravity. The vapor pressure was maintained by the temperature of the cooling water and was measured using a pressure transducer at the vapor tube connected to the condenser.

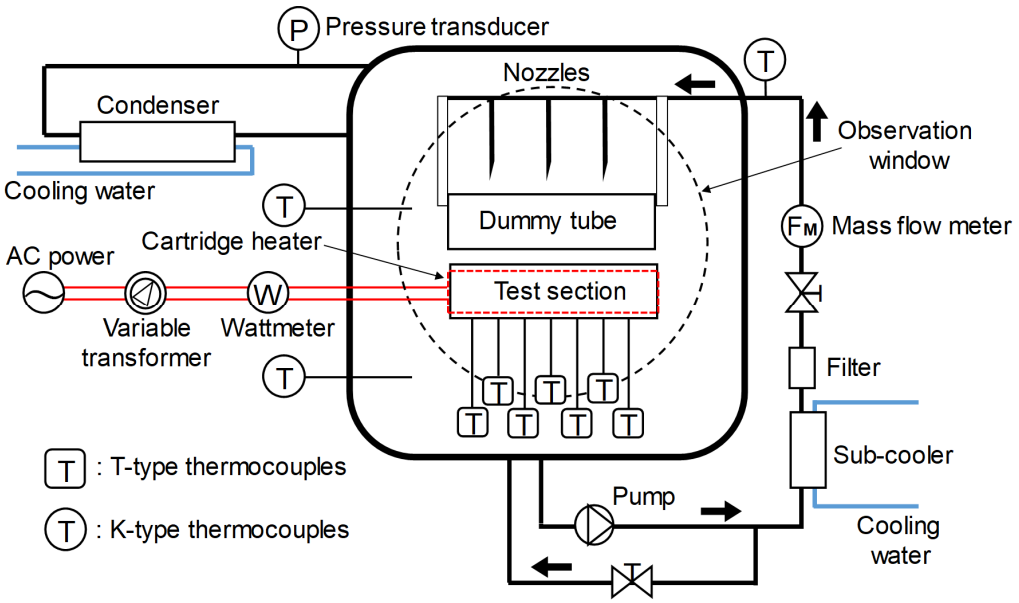

212

213 Fig. 1 Schematic diagram of the experimental apparatus.

214

2.2 Tested tubes

The tested tubes were copper with an outer diameter of 19.05 mm and a length of 50 mm, as shown in Fig. 2. The tube was heated using a cartridge heater inserted along the center axis. The heating length of the heater was equal to the length of the test section. The input power was measured using a wattmeter. The temperature of the heating surface was measured using T-type thermocouples placed at the bottom of the test tube to avoid disturbance of the falling liquid film flow. Constantan wires with a diameter of 0.1 mm were soldered onto the copper wall to form T-type thermocouples.

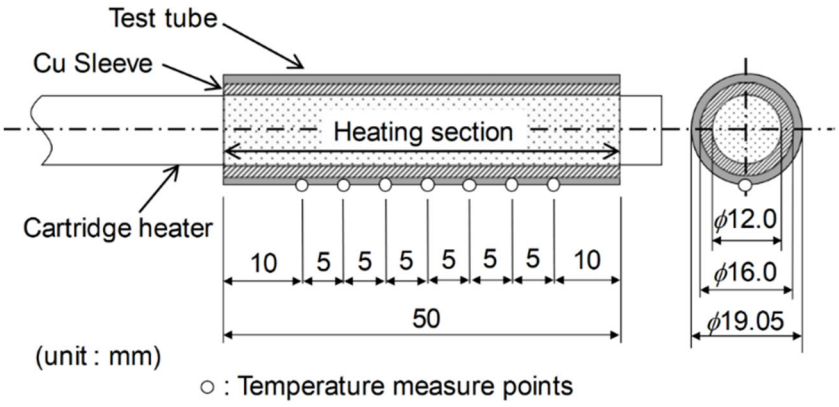

Fig. 2 Details of the test tube.

Thermal spray coating using oxygen-free copper (Cu 99.99 %) as the sprayed material was applied for heat transfer enhancement. The appearance of the thermal spray coated tube is shown in Fig. 3. First, a smooth surface was sandblasted and then coated using an arc wire spraying process in open air. In the arc wire process, two wires of spraying material are melted in a short-circuit arc, and then the melted material is sprayed using compressed air [22]. Figure 4 shows magnified images of the coating. The molten drops were sprayed and stacked randomly. As shown in Fig. 4 (a), cavities of various sizes (up to approximately 50 μm) exist on the surface of the complex multilayer structure. The average surface roughness (*Ra*) and maximum height of profile (*Rz*) were measured using a laser microscope. For the smooth surface, *Ra* = 0.3 μm and *Rz* = 11.7 μm, while for the coated tube *Ra* = 19.4 μm and *Rz* = 171.9 μm.

Fig. 3 Appearance of thermal spray coated tube.

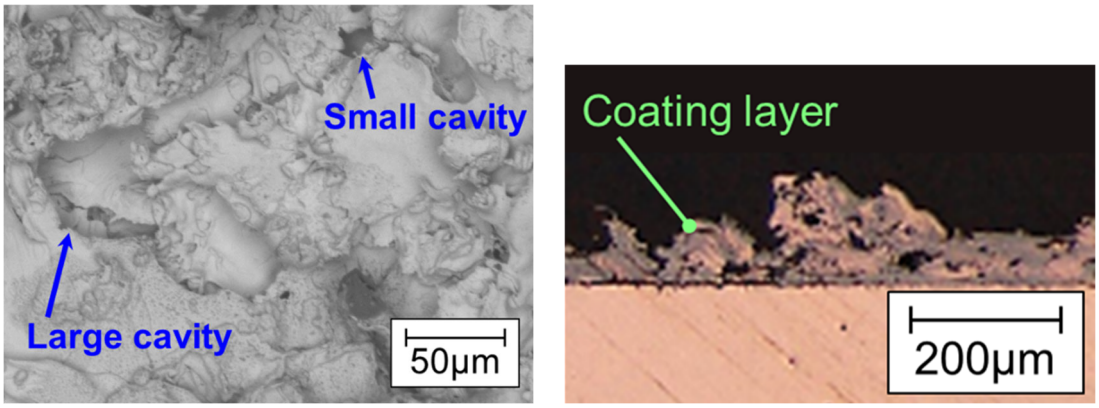

(a) Top view (b) Cross-sectional view

Fig. 4 Magnified images of thermal spray coating.

2.3 Data reduction and uncertainty

The liquid mass flow rate on one side per unit length, Γ, is defined by Eq. (1):

$$\Gamma = \frac{\dot{m}}{2L} \tag{1}$$

The heat flux, $\dot{q}$, is defined for the outer diameter of the base tube using Eq. (2):

$$\dot{q} = \frac{\dot{Q}}{\pi DL} \tag{2}$$

Because the effective heating length of the heater was equal to the length of the test section, the input power measured by the wattmeter was treated as the heating rate.

The heat transfer coefficient, α, is defined by Eq. (3):

$$\alpha = \frac{\dot{q}}{T_{\mathrm{wall}} - T_{\mathrm{sat}}} \tag{3}$$

252

253 The saturation temperature was calculated from the measured pressure using REFPROP version 10.0
254 [23]. The average T_{wall} was obtained from the trimmed average of the seven measured wall
255 temperatures.

256 The uncertainties in the measurements and derived parameters are listed in Table 1. The
257 uncertainties of the saturation temperature for the pressure measurement accuracy of ± 4 kPa was ±
258 0.98 K for R1233zd(E) and ± 0.23 K for R134a. In the calculation of the heat transfer coefficient, the
259 wall temperature measured by each thermocouple was compensated so as the wall superheat of 0 K
260 under the vapor-liquid equilibrium condition without heating. The combined standard uncertainties of
261 the derived parameters, Γ, $\dot{q}$, and α, were evaluated following JCGM 100:2008 [24]. The maximum
262 uncertainty of the heat transfer coefficient was obtained under the lowest heat flux and highest heat
263 transfer coefficient condition using the thermal spray coated tube.

264 The reliability of the measurements was confirmed [14] by comparing the heat transfer coefficient
265 of falling film evaporation on a horizontal smooth tube using R134a with the experimental results of
266 Ribatski and Thome [25].

267 Table 1 Experimental uncertainties.

Parameter	Uncertainty
Temperature, T	± 0.05 K

Mass flow rate, $\dot{m}$	± 4 % R.D.
Pressure, P	± 4 kPa
Input power to the heater, $\dot{Q}$	± 5.5 W
Mass flow rate of liquid film, Γ	± 4 %
Heat flux, $\dot{q}$	± 2–18 %
Heat transfer coefficient, α	± 2–19 %

268

269 **2.4 Experimental conditions**

270 The experiments were conducted at a saturation temperature of 20 °C. The operating pressure was
271 0.108 MPa for R1233zd(E). The liquid film mass flow rate was varied from 8.5×10^{-3} to 6.2×10^{-2}
272 kg/(m·s), and the heat flux was varied from 10 to 85 kW/m^2. The inlet subcooling degree of the
273 refrigerant was maintained within 0.5 K during the falling film evaporation experiments. The behavior
274 of the liquid film on the test section was observed in the horizontal direction through a glass window.

275 The experimental results for R1233zd(E) were compared with those for R134a at the same
276 temperature reported by Ubara et al. [14] to evaluate the effect of the thermophysical properties of the
277 working fluid on the heat transfer characteristics. The main properties of R1233zd(E) and R134a under
278 saturation conditions at 20 °C are listed in Table 2.

279

Table 2 Thermophysical properties of R134a and R1233zd(E) under saturation conditions at 20 °C [23, 26†].

Fluid		R1233zd(E)	R134a
Saturation pressure [MPa] (Reduced pressure [-])		0.108 (0.0298)	0.572 (0.141)
Density [kg/m^3]	Liquid	1275	1225
	Vapor	6.07	27.78
Thermal conductivity (liquid) [mW/(m·K)]		84.25	83.28
Specific heat at constant pressure (liquid) [J/(kg·K)]		1208	1405
Viscosity (liquid) [μPa·s]		300.7	207.4
Latent heat of evaporation [kJ/kg]		193.7	182.3
Surface tension [mN/m]		15.22	8.77
Molar mass [kg/kmol]		130.5	102.0
GWP_{100}† [-]		1	1300

3 Result and discussion

3.1 Pool boiling experiments

Heat transfer in a falling film becomes nucleate boiling dominant at relatively high heat fluxes with a sufficient liquid flow rate. To evaluate the nucleate boiling characteristics, a pool boiling experiment is more suitable than a falling film evaporation experiment because evaporation and forced convection heat transfer effects can be neglected. Therefore, before discussing the falling film evaporation heat transfer, the pool boiling heat transfer characteristics are shown.

3.1.1 Effect of thermophysical properties on the onset of nucleate boiling (ONB)

The activation of nucleation sites was evaluated from the transient changes of the wall superheat in a sudden heating experiment. A sufficiently high heat flux to obtain nucleate boiling on the entire heat transfer surface under steady conditions was suddenly applied. Figures 5 (a) and (b) show the temporal changes in wall superheat against the elapsed time from the start of heating for R1233zd(E) and R134a, respectively. The wall superheat rapidly increased after the heating started and reached a peak, and then rapidly decreased to a certain level. The wall superheats at the peak, $\Delta T_{\mathrm{wall,\,ONB}}$, were 31.1 K for R1233zd(E) and 3.1 K for R134a. A lower value indicates that nucleation sites can be activated by a lower heat flux, and a higher nucleation site density is expected. Therefore, the nucleate boiling heat transfer for R134a was higher than that for R1233zd(E).

The effects of the thermophysical properties of the working fluid on the onset of nucleate boiling were evaluated when considering a theoretical model in the VDI-Wärmeatlas [27]. The relation between ΔT_{wall} and the minimum boiling bubble radius r_{min} is given by Eq. (4) under the assumption that the vapor density is negligibly larger than that of the liquid.

$$\Delta T_{\mathrm{wall}} = \frac{2\sigma T_{\mathrm{sat}}}{\rho_{\mathrm{V}} i r_{\mathrm{min}}} + \frac{r_{\mathrm{min}} \dot{q}}{\lambda_{\mathrm{L}}} \tag{4}$$

Solving for r_{min}, Eq. (5) can be obtained.

$$r_{\min} = \frac{\lambda_L \Delta T_{wall}}{2\dot{q}} \left(1 - \sqrt{1 - \frac{8\sigma \dot{q} T_{sat}}{\rho_V \lambda_L i \Delta T_{wall}^2}} \right) \quad (5)$$

308

309 At the onset of nucleate boiling, r_{min} can be treated as the first activated cavity radius, r_c. The
310 estimated values of r_c from the wall superheat at the ONB were 0.26 μm for R1233zd(E) and 0.35 μm
311 for R134a. These values agreed well with the *Ra* of the smooth tube, and thus, it can be said that the
312 sub-microscale roughness on the tube surface acted as a nucleation site. According to Eq. (4) and the
313 fluid properties summarized in Table 2, it is thought that the difference in the wall superheat at the
314 ONB appeared mainly owing to the difference in vapor density, ρ_V, and surface tension, σ. A lower ρ_V
315 and higher σ lead to a larger difference in the saturation temperature according to the pressure
316 difference between the inside and outside of a vapor bubble. Because the vapor density of R1233zd(E)
317 was 78% lower than that of R134a, and the surface tension was 74% higher, the value of $\Delta T_{wall, ONB}$
318 was higher for R1233zd(E) than for R134a.

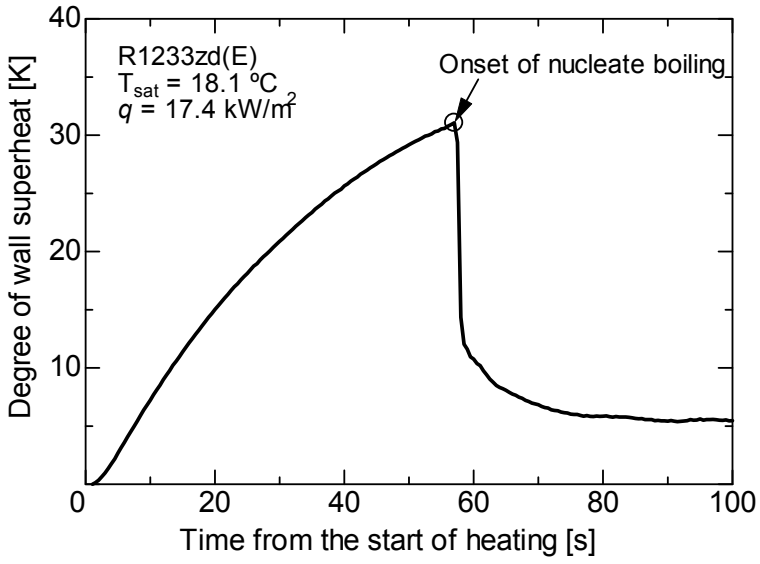

319

320 (a) R1233zd(E)

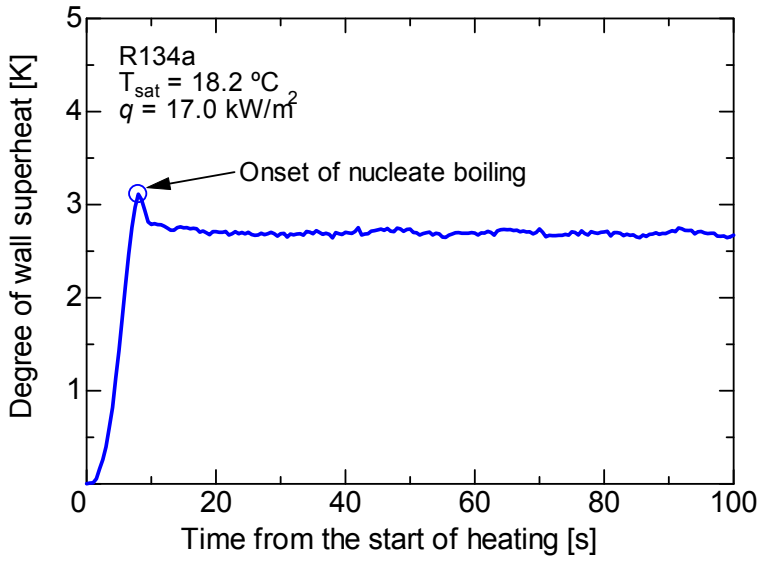

(b) R134a.

Fig. 5 Temporal change of wall superheat in pool boiling with sudden heating.

3.1.2 Pool boiling heat transfer on a smooth tube

The pool boiling heat transfer coefficients are plotted against the heat flux, as shown in Fig. 6. The error bars show the maximum and minimum values of the heat transfer coefficient among the temperature measurement points. Half-filled symbols are the results of Byun et al. [17] at a saturation temperature of 26.7 °C. The results of this study and those of Byun et al. agreed with a deviation of approximately 15 % for R1233zd(E) and approximately 30 % for R134a. The broken and chain lines show the correlation of the pool boiling heat transfer coefficient around a smooth horizontal tube proposed by Jung et al. [28] for R1233zd(E) and R134a, respectively. Jung's correlation is expressed in Eq. (6), (7), and (8). The heat flux range of the experimental data used for the development of the correlation ranged from 10 to 80 kW/m^2. The equations include several thermophysical properties,

such as the surface tension and vapor density, which influence bubble nucleation, as described in Section 3.1.1.

$$\alpha = 10\frac{\lambda_{\mathrm{L}}}{D_{\mathrm{b}}}\left(\frac{\dot{q}D_{\mathrm{b}}}{\lambda_{\mathrm{L}}T_{\mathrm{sat}}}\right)^{C}\left(\frac{P_{\mathrm{sat}}}{P_{\mathrm{crt}}}\right)^{0.1}\left(1-\frac{T_{\mathrm{sat}}}{T_{\mathrm{crt}}}\right)^{-1.4}\left(\frac{\mu_{\mathrm{L}}c_{p_{\mathrm{L}}}}{\lambda_{\mathrm{L}}}\right)^{-0.25} \quad (6)$$

$$D_b = 0.511\sqrt{\frac{2\sigma}{g(\rho_{\mathrm{L}}-\rho_{\mathrm{V}})}} \quad (7)$$

$$C = 0.855\left(\frac{\rho_{\mathrm{V}}}{\rho_{\mathrm{L}}}\right)^{0.309}\left(\frac{P_{\mathrm{sat}}}{P_{\mathrm{crt}}}\right)^{-0.437} \quad (8)$$

Although the experimental results were approximately 35% higher than the predicted values for most of the conditions, the gradient of the curves showed good agreement. In addition, the heat transfer coefficients for R134a were approximately 2.5 times higher than those for R1233zd(E) in both the predicted and experimental results. It can be stated that the effects of the heat flux and thermophysical properties on the nucleate boiling heat transfer were expressed through Jung's correlation.

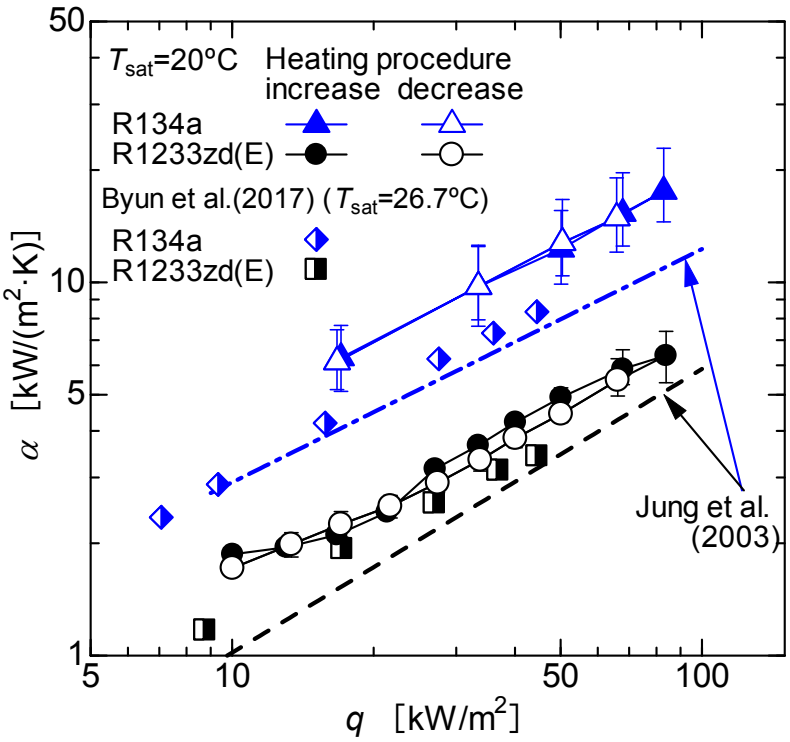

Fig. 6 Pool boiling heat transfer coefficients on a smooth surface for R134a and R1233zd(E).

3.1.3 Effects of thermal spray coating

The pool boiling heat transfer coefficients of the thermal spray coating are shown in Fig. 7. For R1233zd(E), the heat transfer coefficients for the coating were twice those of the smooth tube. Numerous cavities on the thermal coating surface resulted in a high nucleate site density. The gradient of the curve for the coated tube was constant and almost the same as that for the smooth tube. The difference in heat transfer coefficients between the process of increasing and decreasing the heat flux was slight, whereas a large hysteresis effect was observed for R134a on the coating surface.

The main cause may be the difference in the ONB characteristics mentioned in Section 3.1.1. Although many cavities exist on the coated surface, activation of the nucleation sites requires a higher

wall superheat for R1233zd(E) than for R134a. Therefore, not all cavities activated in R134a can be activated in R1233zd(E) owing to an insufficient wall superheat.

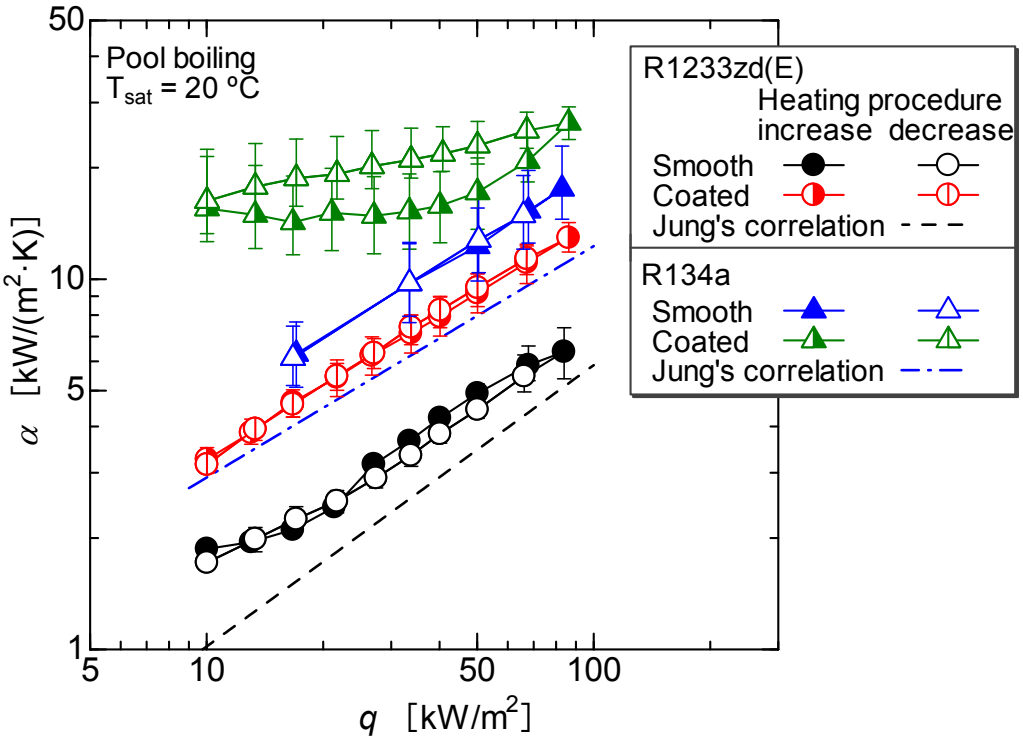

Fig. 7 Effect of heating surface structure on pool boiling heat transfer.

3.2 Falling film evaporation

3.2.1 Effect of liquid film flow rate

Figure 8 shows the experimental results of the heat transfer coefficient against the liquid film mass flow rate per unit length. At a heat flux of 50.1 kW/m^2 with a minimum Γ of 8.5 × 10^{-3} kg/(m·s), the entire surface of both tubes was dried out, and the wall temperatures increased significantly.

For the smooth tube, at a heat flux of 16.7 kW/m^2, the heat transfer coefficient increased with an increase in the liquid film flow rate over the experimental range owing to the improvement in forced

convective heat transfer. Nucleate boiling may not be active at a low heat flux. Similar results were reported by Jin et al. [29] at a heat flux of 10 kW/m^2 using R600a as the working fluid. At higher heat fluxes of 33.4 and 50.1 kW/m^2, the heat transfer coefficients were insensitive to film flow rate changes when $\Gamma > 3.0\times 10^{-2}$ kg/(m·s). This behavior is known as the plateau stage and has been observed in several studies, including those by Zhao et al. [5] and Bock et al. [6]. Active nucleate boiling in the liquid film was dominant during heat transfer. In addition, when the liquid flow rate is sufficiently high, it is expected that vapor bubbles leading to a superficial increase in the volumetric film flow rate promote the spreading of the liquid film.

For the thermal spray coated tube, the heat transfer coefficients were higher than those for the smooth tube. At a heat flux of 16.7 kW/m^2, the values were mostly constant over the experimental range. Nucleation sites on the thermal spray coating could be activated with a lower heat flux than with a smooth tube, and the heat transfer was dominated by nucleate boiling. At 33.4 kW/m^2, the heat transfer coefficient increased to below $\Gamma = 1.7 \times 10^{-2}$ kg/(m·s) and became constant above that value. At 50.1 kW/m^2, a transition to the nucleate boiling dominant region was observed at $\Gamma = 2.8 \times 10^{-2}$ kg/(m·s).

The film flow rate at the transition to the nucleate boiling dominant region was lower for the coated surface than for the smooth surface. A similar tendency was reported in our previous study [14] using R134a. The fine porous structure of the thermal spray coating enhanced the liquid spread and bubble nucleation in the liquid film. Focusing on cases with flow rates lower than the threshold, the decreasing

388 rate of the heat transfer coefficient with decreasing liquid film flow rate became larger with increasing
389 heat flux. On the coated surface, a thinner liquid film spread by capillary force could easily dry out
390 because of the high heat flux.
391

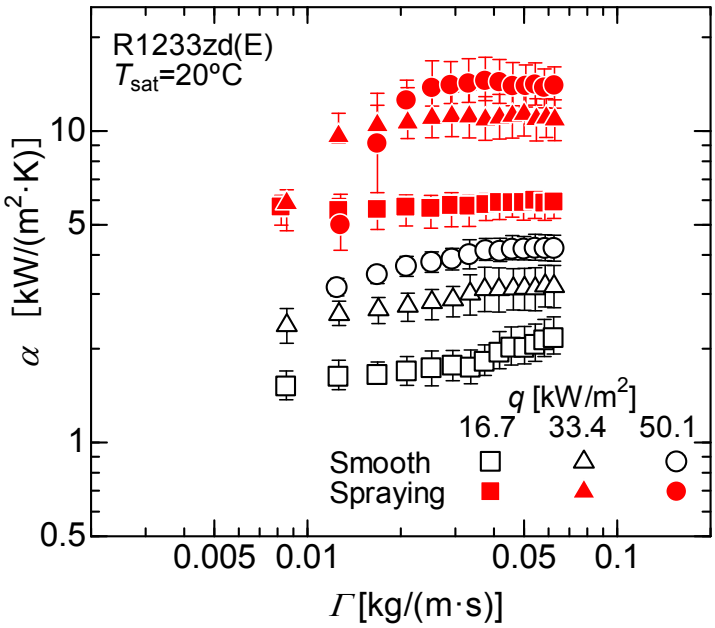

392

393 Fig. 8 Heat transfer coefficient of falling film evaporation against film mass flow rate.

394

395 **3.2.2 Effect of the heat flux and heating history**

396 Figure 9 shows falling film flow behaviors at Γ = 0.033 kg/(m·s) without heating. Liquid flowed
397 down as a uniform and continuous sheet to the top of the test tube through a narrow gap. It was
398 confirmed that the entire heat transfer surface was covered by a film under this condition. Figure 10
399 shows the falling film evaporation heat transfer coefficients against a heat flux for the film flow rate

400 at 0.033 kg/(m·s). The broken line shows the correlation of pool boiling heat transfer around a
401 horizontal smooth tube as proposed by Jung et al. [28].

402 For the smooth tube, the gradient of the curve agreed well with that for pool boiling heat transfer
403 at a heat flux of less than 50.0 kW/m^2. It can be said that the heat transfer was dominated by nucleate
404 boiling in the liquid film because the film flow rate was sufficient to cover the heat transfer surface, as
405 shown in Fig. 9. However, at heat fluxes above 50.0 kW/m^2, a deterioration in the heat transfer
406 coefficient was observed. Fujita and Tsutsui [2] and Ribatski and Thome [3] reported that the
407 appearance of dry patches did not directly cause the deterioration of the heat transfer coefficient. In
408 addition, in this study, most of the dry patches were not fixed and did not drastically expand with
409 increasing heat flux at less than 50.0 kW/m^2. Figure 11 (a) shows the falling film evaporation behavior
410 at a low heat flux of 22.1 kW/m^2 during the increasing process. Stable dry patches were observed only
411 at the bottom of both ends of the test section. When the heat flux exceeded 50.0 kW/m^2, stable dry
412 patches obviously expanded, as shown at the highest heat flux of 78.2 kW/m^2 in Fig. 11 (b). It should
413 be mentioned that, during the experimental operation, the heat flux was once set to over 80 kW/m^2,
414 and after increasing the wall temperature owing to a full dry out, the heat flux was reduced to 78.2
415 kW/m^2. As shown in Fig. 10, the heat transfer coefficients in the decreasing heat flux process were
416 slightly lower than those in the increasing process. The difference was obvious at a high heat flux,
417 where the deterioration in the heat transfer coefficient was observed. Because the advancing contact
418 angle for rewetting is larger than the receding contact angle, dry patches formed at a high heat flux

could remain and cause deterioration. However, the difference was minimal below 40 kW/m^2. Further analysis is required to clarify the hysteresis effect. Figure 11 (c) shows the evaporation behavior at 21.7 kW/m^2 in the decreasing process. Comparing Fig. 11 (c) with (a), no clear differences in the boiling behaviors, such as dry patch formation or bubble distribution, were observed.

The thermal spray coated tube produced higher heat transfer coefficients than the smooth tube over the experimental heat flux range, as shown in Fig. 10. During the process of increasing the heat flux, the heat transfer coefficient monotonically increased with increasing heat flux. An obvious deterioration of the heat transfer coefficient at high heat flux, as seen in the smooth tube, did not appear because the high wickability of the rough structure was effective for spreading the liquid. Figure 12 (a) shows the evaporation behavior at a low heat flux of 22.1 kW/m^2 during the increasing process. Dry stable areas, as shown on the smooth tube in Fig. 11 (a), did not appear on the coated tube. At the highest heat flux of 84.2 kW/m^2, as shown in Fig. 12 (b), a dry patch was observed on the left half of the test section. However, compared with the smooth tube (Fig. 11 (b)), it is obvious that the liquid film spread wider on the coated surface than on the smooth surface, even at a slightly higher heat flux. In the decreasing heat flux process shown in Fig. 10, the heat transfer coefficient was improved at a heat flux of 66.2 kW/m^2, and then decreased with almost the same gradient as the smooth tube. In contrast to the smooth tube, the heat transfer coefficients were higher during the decreasing process than during the increasing process. Figure 12 (c) shows the evaporation behavior at a heat flux of 21.7 kW/m^2 during the decreasing process. The number of bubbles in the liquid film was larger than that

438 during the increasing process (Fig. 12 (a)). Because many cavities on the porous coating surface were

439 activated at the highest heat flux, the density of the nucleation sites increased during the decreasing

440 process.

441

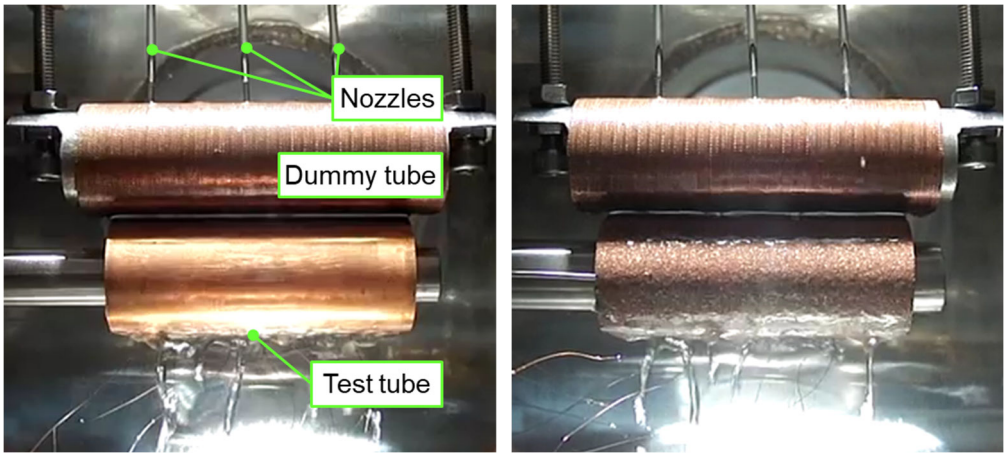

(a) smooth tube (b) thermal spray coated tube

442 Fig. 9 Falling film flow behaviors at Γ = 0.033 kg/(m·s) without heating.

443

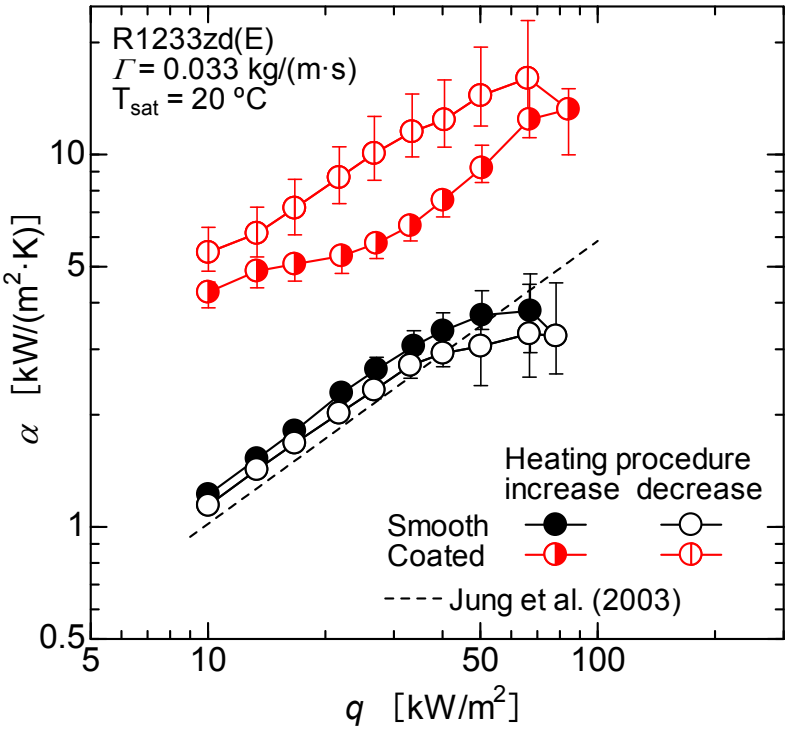

444

445 Fig. 10 Effect of heat flux and heating history on heat transfer coefficient of falling film evaporation

446 using R1233zd(E).

447

448

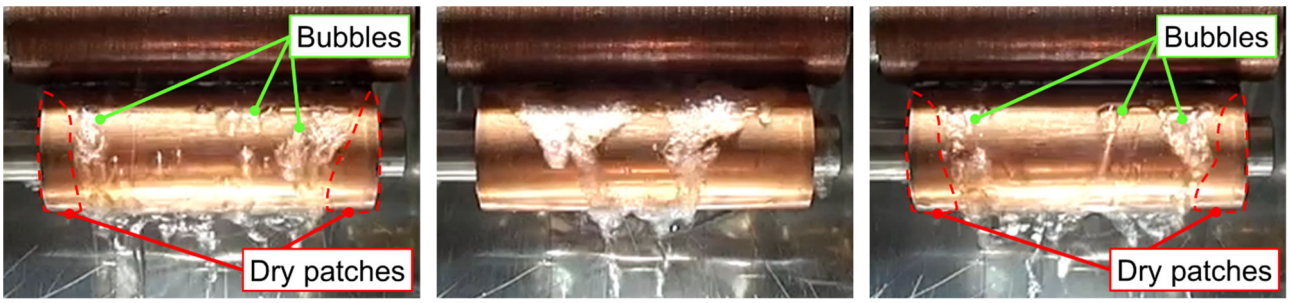

(a) 22.1 kW/m^2, increasing (b) 78.2 kW/m^2, decreasing (c) 21.7 kW/m^2, decreasing

449 Fig. 11 Falling film evaporation behaviors on the smooth tube at Γ = 0.033 kg/(m·s).

450

(a) 22.1 kW/m^2, increasing (b) 84.2 kW/m^2, increasing (c) 21.7 kW/m^2, decreasing

Fig. 12 Falling film evaporation behaviors on the thermal spray coated tube at Γ = 0.033 kg/(m·s).

3.2.3 Comparison with pool boiling heat transfer

A comparison of the heat transfer coefficients between falling film evaporation and pool boiling for the smooth and the thermal spray coated tubes is shown in Figs. 13 (a) and (b), respectively.

For the smooth tube in Fig. 13 (a), the heat transfer coefficients in pool boiling were slightly higher than those in falling film evaporation. Both heat transfer modes were dominated by nucleate boiling, but heat transfer deterioration owing to the dry patches occurred during the falling film evaporation. Under high heat flux conditions, the difference increased.

For the coated surface in Fig. 13 (b), the hysteresis effect of the heating procedure appeared only during falling film evaporation. The heat transfer coefficients were higher for falling film evaporation than for pool boiling during the heat flux decreasing process. At a high heat flux, nucleation sites may be more easily activated during falling film evaporation. Because small dry patches were randomly formed on the surface during falling film evaporation, the vapor remaining in the cavities may activate nucleation sites.

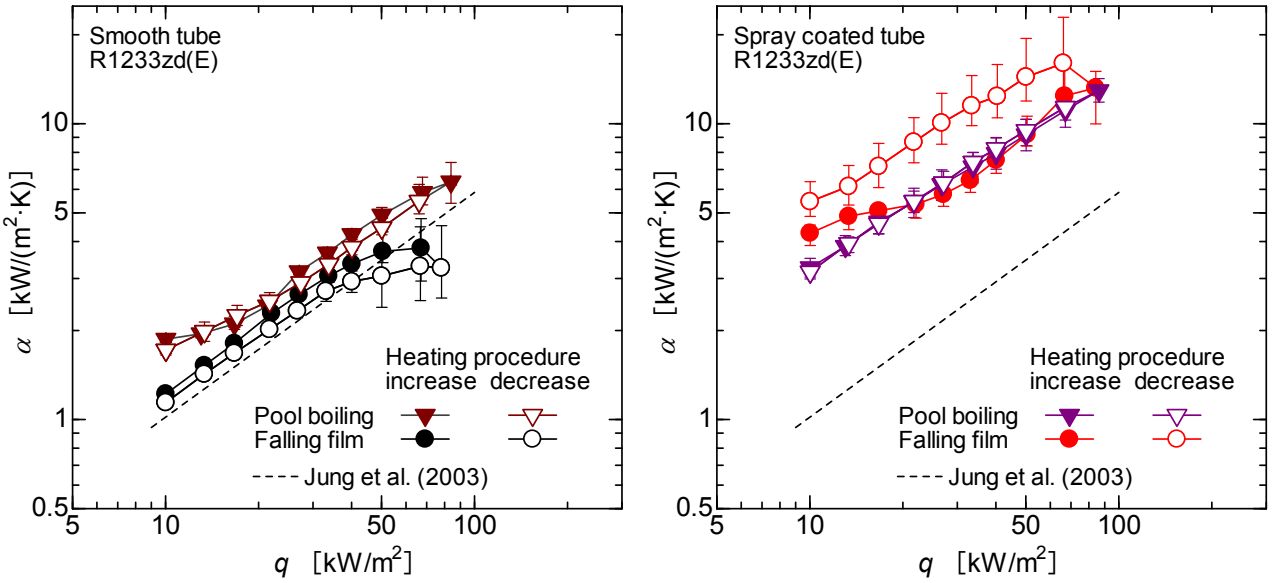

(a) Smooth tube (b) Thermal spray coated tube

Fig. 13 Comparison in heat transfer coefficient between falling film evaporation and pool boiling.

3.2.4 Comparison with the results for R134a

Figure 14 shows the heat transfer coefficients of falling film evaporation for R1233zd(E) compared with those for R134a reported by Ubara et al. [14]. For the smooth tube, the deterioration in the heat transfer coefficient at a high heat flux was larger for R1233zd(E) than for R134a. Because the wall superheat for R1233zd(E) was higher than that for R134a, the edge of the liquid film could evaporate rapidly and large dry patches may be formed. This caused a weak spreading of the liquid film. It should be noted that the effect of thermophysical properties and surface structure on the spreading of liquid film with nucleate boiling has not been yet fully understood, so further investigations such as contact angle measurement, flow observation with high spatial and time resolutions, using various fluids under various saturation temperature conditions are needed. The difference in the heat transfer coefficients

between the two refrigerants agreed with the difference in the predicted values based on Jung's correlation for pool boiling. Therefore, the heat transfer coefficient of falling film evaporation can be predicted based on a prediction method for nucleate boiling heat transfer.

For the thermal spray coated tube, R134a also showed a higher heat transfer coefficient, as shown for the smooth tube. However, the trend of the heat transfer coefficient with respect to the heat flux was different. R1233zd(E) exhibited a larger hysteresis effect in the heat transfer coefficient. In addition, whereas the gradient in the heat flux decreasing process for R1233zd(E) agreed well with Jung's correlation, that for R134a was smaller. For R134a, further heat transfer enhancement could be obtained owing to a larger nucleation site density and the resulting strong agitation in the liquid film.

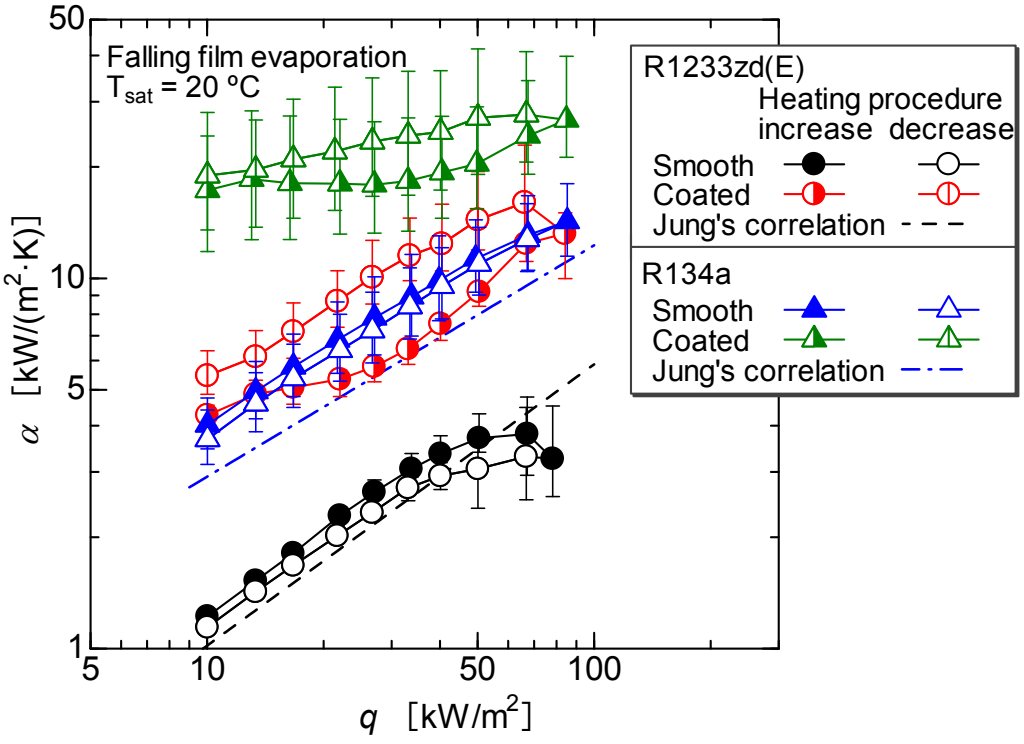

Fig. 14 Comparison of falling film evaporation heat transfer coefficients between R1233zd(E) and R134a at Γ = 0.033 kg/(m·s) on the smooth and the thermal spray coated tubes.

An enhancement of the heat transfer from the smooth tube to the thermal spray coated tube is shown in Fig. 15. For R1233zd(E), the highest value was 4.8 at heat fluxes of 10.0 and 66.2 kW/m^2. The larger enhancement factor at a low heat flux during the decreasing process may be due to the larger nucleation site density activated at the high heat flux. In contrast, the enhancement at a high heat flux may be due to the suppression of dry patch formation. Compared with the values for R134a, a larger enhancement factor was obtained for R1233zd(E) at a heat flux of over 30 kW/m^2. As shown in Fig. 14, for a smooth surface, the heat transfer coefficient deteriorated only for R1233zd(E). This deterioration may be caused by dry patch formation. Thus, the promotion of the spreading of the liquid by the rough coating structure was more effective for R1233zd(E) than for R134a.

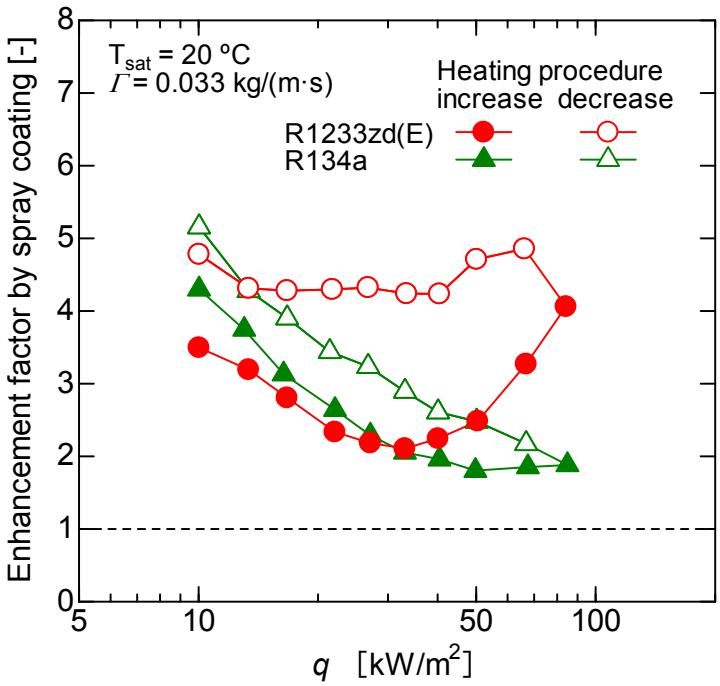

Fig. 15 Heat transfer enhancement factor by the thermal spray coating.

4 Conclusion

The falling film evaporation and pool boiling heat transfer coefficients of R1233zd(E) on a single horizontal tube were experimentally evaluated. The thermal spray coated tube, which is a novel heat transfer enhancement surface applicable to super-hard metal tubes, was tested in addition to the smooth surface. The effects of the refrigerant flow rate, heat flux, heating history, and surface structure of the thermal spray coating are discussed. The results were also compared with those of R134a to evaluate the effect of the thermophysical properties of the working fluid. The main conclusions are summarized as follows:

- R1233d(E) required a higher wall superheat for the onset of nucleate boiling than R134a owing to the higher surface tension and lower vapor density. As a result, R1233zd(E) produced lower pool boiling heat transfer coefficients.
- R1233d(E) produced lower falling film evaporation heat transfer coefficients than R134a. Because nucleate boiling dominated the heat transfer in the liquid film, the difference was due to the higher wall superheat to activate bubble nucleation.
- With a sufficient liquid film flow rate and heat flux, the heat transfer in the liquid film became nucleate boiling dominant. Vapor bubbles in the liquid film may promote stable film formation because of the increase in the superficial liquid film thickness and flow resistance.
- The thermal spray coated surface enhanced liquid spreading and nucleate boiling. Nucleate boiling occurred at a lower liquid film flow rate and produced higher heat transfer coefficients

than the smooth tube. The heat transfer enhancement factor due to the thermal spray coating was 2.1–4.8 times.

- The effect of the heating history was small for the smooth tube, whereas the heat transfer coefficients were higher in the heat flux decreasing process for the coated tube. The hysteresis effect was observed only for falling film evaporation. Cavities in the porous coating layer could be activated by dry patches moving randomly on the heat transfer surface at the highest heat flux.

Acknowledgements

The authors thank TOCALO Co., Ltd. for processing the thermal spray coating.

Funding

This research did not receive any specific grants from funding agencies in the public, commercial, or not-for-profit sectors.

References

[1] G. Ribatski, A.M. Jacobi, Falling-film evaporation on horizontal tubes—a critical review. Int. J. Refrig. 28 (2005) 635–653. https://doi.org/10.1016/j.ijrefrig.2004.12.002

[2] Y. Fujita, M. Tsutsui, Experimental investigation of falling film evaporation on horizontal tubes. Heat Transf. Jpn. Res. 27 (1998) 609–618. https://doi.org/10.1002/(SICI)1520-6556(1998)27:8%3C609::AID-HTJ5%3E3.0.CO;2-N

[3] G. Ribatski, J.R. Thome, 2005. A visual study of R134a falling film evaporation on enhanced and plain tubes, in: International Symposium on Multiphase Flow, Heat Mass Transfer and Energy Conservation.

[4] C.Y. Zhao, W.T. Ji, P.H. Jin, W.Q. Tao, Heat transfer correlation of the falling film evaporation on a single horizontal smooth tube, Appl. Therm. Eng. 103 (2016) 177–186. https://doi.org/10.1016/j.applthermaleng.2016.02.090

[5] C.Y. Zhao, P.H. Jin, W.T. Ji, Y.L. He, W.Q. Tao, Experimental investigations of R134a and R123 falling film evaporation on enhanced horizontal tubes. Int. J. Refrig. 75 (2017) 190–203. https://doi.org/10.1016/j.ijrefrig.2016.12.013

[6] B.D. Bock, J.P. Meyer, J.R. Thome, 2019. Falling film boiling and pool boiling on plain circular tubes: Influence of surface roughness, surface material and saturation temperature on heat transfer and dryout. Exp. Therm. Fluid Sci. 109, 109870. https://doi.org/10.1016/j.expthermflusci.2019.109870

564 [7] D. Jige, H. Miyata, N. Inoue, Falling film evaporation of R1234ze(E) and R245fa on a horizontal
565 smooth tube. Exp. Therm. Fluid Sci. 105 (2019) 58–66.
566 https://doi.org/10.1016/j.expthermflusci.2019.03.012

567

568 [8] H. Asano, K. Akita, M. Inoue, Effect of gravity on pool boiling heat transfer on thermal spray
569 coating. Microgravity Sci. Technol. 19 (2007) 90–92. https://doi.org/10.1007/BF02915762

570

571 [9] A. K. Dewangan, A. Kumar, R. Kumar, Experimental study of nucleate boiling heat transfer of R-
572 134a and R-600a on thermal spray coating surfaces. Int. J. Therm. Sci. 110 (2016) 304–313.
573 https://doi.org/10.1016/j.ijthermalsci.2016.07.015

574

575 [10] J. Tehver, H. Sui, V. Temkina, Heat transfer and hysteresis phenomena in boiling on porous
576 plasma-sprayed surface, Exp. Therm. Fluid Sci. 5 (1992) 714–727. https://doi.org/10.1016/0894-
577 1777(92)90115-L

578

579 [11] R. Abraham, A. Mani, 2018. Flame spray coating on horizontal tubes for enhancement of falling
580 film evaporation in multi-effect distillation system, in: 9th Asian Thermal Spray Conference
581 (ATSC-2018), Paper ID: ATSC-1085.

582

583 [12] N. Bogan, C. Park, Influences of solution subcooling, wall superheat and porous-layer coating on
584 heat transfer in a horizontal-tube, falling-film heat exchanger. Int. J. Heat Mass Transf. 68 (2014)
585 141–150. https://doi.org/10.1016/j.ijheatmasstransfer.2013.09.005

586

587 [13] A.M. Abed, M.A. Alghoul, M.H. Yazdi, A.N. Al-Shamani, K. Sopian, The role of enhancement
588 techniques on heat and mass transfer characteristics of shell and tube spray evaporator: A detailed
589 review. Appl. Therm. Eng. 75 (2015) 923–940.
590 https://doi.org/10.1016/j.applthermaleng.2014.10.020

591

592 [14] T. Ubara, H. Asano, K. Sugimoto, 2020. Heat transfer enhancement of falling film evaporation
593 on a horizontal tube by thermal spray coating. Appl. Sci. 10, 1632.
594 https://doi.org/10.3390/app10051632

595

596 [15] L.H. Chien, Y.L. Tsai, An experimental study of pool boiling and falling film vaporization on
597 horizontal tubes in R-245fa. Appl. Therm. Eng. 31 (2011) 4044–4054.
598 https://doi.org/10.1016/j.applthermaleng.2011.08.007

599

600 [16] R. Nagata, C. Kondou, S. Koyama, Comparative assessment of condensation and pool boiling
601 heat transfer on horizontal plain single tubes for R1234ze(E), R1234ze(Z), and R1233zd(E). Int.
602 J. Refrig. 63 (2016) 157–170. https://doi.org/10.1016/j.ijrefrig.2015.11.002

603

604 [17] H.W. Byun, D.H. Kim, S.H. Yoon, C.H. Song, K.H. Lee, O.J. Kim, Pool boiling performance of
605 enhanced tubes on low GWP refrigerants, Appl. Therm. Eng. 123 (2017) 791–798.
606 https://doi.org/10.1016/j.applthermaleng.2017.05.009

607

608 [18] W.T. Ji, S.M. Xiong, L. Chen, C.Y. Zhao, W.Q. Tao, Effect of subsurface tunnel on the nucleate
609 pool boiling heat transfer of R1234ze(E), R1233zd(E) and R134a, Int. J. Refrig. 122 (2021) 122–
610 133. https://doi.org/10.1016/j.ijrefrig.2020.11.002

611

612 [19] M. Welzl, F. Heberle, D. Brüggemann, Experimental evaluation of nucleate pool boiling heat
613 transfer correlations for R245fa and R1233zd(E) in ORC applications. Renew. Energy 147 (2020)
614 2855–2864. https://doi.org/10.1016/j.renene.2018.09.093

615

616 [20] M. Hassani, R. Kouhikamali, Heat and mass transfer modeling of R-245fa and R1233zd(E) with
617 concurrent boiling and convective evaporation in falling film applications. Int. J. Refrig. 117
618 (2020) 181–189. https://doi.org/10.1016/j.ijrefrig.2020.05.002

619

620 [21] Q. Wang, M. Li, W. Xu, L. Yao, X. Liu, D. Su, P. Wang, 2020. Review on liquid film flow and
621 heat transfer characteristics outside horizontal tube falling film evaporator: Cfd numerical
622 simulation. Int. J. Heat Mass Transf. 163, 120440.
623 https://doi.org/10.1016/j.ijheatmasstransfer.2020.120440

624

625 [22] TOCALO Co., Ltd., Electric Arc Spraying Process (Arc Process) / Technologies.
626 https://www.tocalo.co.jp/english/technical/arc.html, (accessed 6 May 2021).

627

628 [23] E.W. Lemmon, I.H. Bell, M.L. Huber, M.O. McLinden, 2018. NIST Standard Reference Database
629 23: Reference Fluid Thermodynamic and Transport Properties-REFPROP, Version 10.0,
630 National Institute of Standards and Technology. https://doi.org/10.18434/T4/1502528

631

632 [24] JCGM 100:2008, 2008. Evaluation of measurement data — Guide to the expression of uncertainty
633 in measurement. BIPM Joint Committee for Guides in Metrology, Paris.
634 https://www.bipm.org/utils/common/documents/jcgm/JCGM_100_2008_E.pdf
635

636 [25] G. Ribatski, J.R. Thome, Experimental study on the onset of local dryout in an evaporating falling
637 film on horizontal plain tubes, Exp. Therm. Fluid Sci. 31 (2007) 483–493.
638 https://doi.org/10.1016/j.expthermflusci.2006.05.010

639

640 [26] Intergovernmental Panel on Climate Change, Climate Change 2013 – The Physical Science Basis:
641 Working Group I Contribution to the Fifth Assessment Report of the Intergovernmental Panel on
642 Climate Change, Cambridge University Press, Cambridge, 2014, 731–732.
643

644 [27] J.J. Schröder, Behältersieden unterkühlter Flüssigkeiten (Sieden bei freier Konvektion), in: VDI-
645 GVC (Ed.), VDI-Wärmeatlas 10. Auflage, Springer Berlin Heidelberg, Berlin, 2006, Section Haa.
646

647 [28] D. Jung, Y. Kim, Y. Ko, K. Song, Nucleate boiling heat transfer coefficients of pure halogenated
648 refrigerants. Int. J. Refrig. 26 (2003) 240–248. https://doi.org/10.1016/S0140-7007(02)00040-3

649

650

[29] P.H. Jin, Z. Zhang, I. Mostafa, C.Y. Zhao, W.T. Ji, W.Q. Tao, Heat transfer correlations of refrigerant falling film evaporation on a single horizontal smooth tube. Int. J. Heat Mass Transf. 133 (2019) 96–106. https://doi.org/10.1016/j.ijheatmasstransfer.2018.12.053